The American Journal of Pathology, Vol. 180, No. 2, February 2012
Copyright © 2012 American Society for Investigative Pathology.
Published by Elsevier Inc. All rights reserved.
DOI: 10.1016/j.ajpath.2011.10.011

Cardiovascular, Pulmonary, and Renal Pathology

Development of Oxidative Stress in the Peritubular Capillary Microenvironment Mediates Sepsis-Induced Renal Microcirculatory Failure and Acute Kidney Injury

Zhen Wang,* Joseph H. Holthoff,* Kathryn A. Seely,* Elina Pathak,* Horace J. Spencer III,† Neriman Gokden,‡ and Philip R. Mayeux*

From the Departments of Pharmacology and Toxicology, Biostatistics,† and Pathology,‡ University of Arkansas for Medical Sciences, Little Rock, Arkansas*

Acute kidney injury is a frequent and serious complication of sepsis. To better understand the development of sepsis-induced acute kidney injury, we performed the first time-dependent studies to document changes in renal hemodynamics and oxidant generation in the peritubular microenvironment using the murine cecal ligation and puncture (CLP) model of sepsis. CLP caused an increase in renal capillary permeability at 2 hours, followed by decreases in mean arterial pressure, renal blood flow (RBF), and renal capillary perfusion at 4 hours, which were sustained through 18 hours. The decline in hemodynamic parameters was associated with hypoxia and oxidant generation in the peritubular microenvironment and a decrease in glomerular filtration rate. The role of oxidants was assessed using the superoxide dismutase mimetic/peroxynitrite scavenger MnTMPyP [Mn(III)tetrakis(1-methyl-4-pyridyl)porphyrin]. At 10 mg/kg administered 6 hours after CLP, MnTMPyP did not alter blood pressure, but blocked superoxide and peroxynitrite generation, reversed the decline in RBF, capillary perfusion, and glomerular filtration rate, preserved tubular architecture, and increased 48-hour survival. However, MnTMPyP administered at CLP did not prevent capillary permeability or the decrease in RBF and capillary perfusion, which suggests that these early events are not mediated by oxidants. These data demonstrate that renal hemodynamic changes occur early after sepsis and that targeting the later oxidant generation can break the cycle of injury and enable the microcirculation and renal function to recover. ***(Am J Pathol 2012, 180:505–516; DOI: 10.1016/j.ajpath.2011.10.011)***

Acute kidney injury (AKI) is one of the most serious complications of sepsis because it worsens prognosis and increases cost of care. The incidence of AKI increases with the severity of sepsis and the mortality for septic patients with AKI is approximately doubled to near 70% compared with patients with sepsis alone.[1] It is estimated that AKI develops within the first 24 hours in 64% of patients with sepsis with hypotension.[2] Thus, protecting the kidney during sepsis could significantly reduce morbidity and mortality in patients with severe sepsis. Treatment of sepsis and especially of sepsis-induced AKI has advanced little during the last several decades.[3] The standard of care is primarily supportive, with fluid resuscitation, broad-spectrum antibiotic therapy, lung-protective ventilation, and, if necessary, dialysis. Treatment is approached in two phases: resuscitation within the first 6 hours and management within the first 24 hours, and has improved survival, although mortality remains high.[4]

A barrier to uncovering new specific therapeutic approaches for sepsis-induced AKI is lack of understanding of the temporal and mechanistic relationships between the changes in renal hemodynamics, peritubular microcirculatory dysfunction, and renal tubular injury. These are critical issues because, in general, the severity of microvascular dysfunction correlates with patient mortality,[5,6] and the timing of treatment, especially regarding

Supported by NIH grants R01 DK075991 (P.R.M.), R01 DK075991-S1 (K.A.S.), and F30 DK085705 (J.H.H.), American Heart Association grant 10PRE4140065 (Z.W.), and UAMS Translational Research Institute supported by NIH National Center for Research Resources grant UL1 RR029884 (H.J.S.).

Accepted for publication October 17, 2011.

Address reprint requests to Philip R. Mayeux, Ph.D., Department of Pharmacology and Toxicology, University of Arkansas for Medical Sciences, 4301 W Markham St, No. 611, Little Rock, AR 72205. E-mail: prmayeux@uams.edu.

the development of AKI, is well recognized as critical to its success.[7] To help address this need, we performed a detailed time course study to characterize the development of microvascular dysfunction during sepsis-induced AKI using the clinically relevant cecal ligation and puncture (CLP) model in aged mice.[8]

It is becoming increasingly clear that oxidative stress and microvascular dysfunction have important roles in the development of multiple-organ failure during sepsis.[9,10] Severely ill patients with sepsis demonstrate increased oxidative stress markers[11,12] and reduced microvascular perfusion.[13] The role of oxidants in sepsis-induced AKI is supported by animal studies in which inhibiting NO-derived reactive nitrogen species (RNS) such as peroxynitrite (the product of NO and superoxide) reduces tubular injury and preserves renal function in both lipopolysaccharide and CLP models of sepsis.[14–16] However, the relationship between renal microvascular changes and oxidant generation has not been directly studied. To investigate this, the therapeutic potential of the superoxide dismutase mimetic and peroxynitrite scavenger MnTMPyP [Mn(III)tetrakis(1-methyl-4-pyridyl) porphyrin, tetratosylate, hydroxide][17,18] was evaluated in the CLP model using a delayed dosing protocol.

Materials and Methods

Materials

Fluorescein isothiocyanate–dextran 500,000 Da conjugate (FITC-dextran), FITC-inulin, xanthine, xanthine oxidase, cytochrome *c*, and Evans Blue dye were purchased from Sigma-Aldrich Corp. (St. Louis, MO). 2-(3,6-Diamino-9H-xanthen-9-yl)–benzoic acid, methyl ester [dihydrorhodamine 123 (DHR-123)], and MitoSOX Red were purchased from Invitrogen Corp. (Eugene, OR). MnTMPyP was purchased from EMD-Calbiochem (La Jolla, CA).

Mouse Model of CLP-Induced AKI

Sepsis was CLP-induced as described previously.[14] Male C57/BL6 mice (Harlan Laboratories, Inc., Indianapolis, IN) at 39 to 40 weeks of age were acclimated for 1 week with free access to food and water. At surgery, the mice were anesthetized via isoflurane inhalation. After laparotomy, a 4–0 silk ligature was placed 1.5 cm from the cecal tip. The cecum was punctured twice using a 21-gauge needle and gently squeezed to express an approximately 1-mm column of fecal material (CLP mice). In sham-operated mice (Sham), the cecum was located but neither ligated nor punctured. The abdominal incision was closed in two layers using 4–0 silk sutures. After surgery, 1 mL warmed normal saline solution was administered into the intraperitoneal cavity. Mice were then placed in individual cages and set on a warming pad. Mice studied at 18 hours after CLP received imipenem-cilastatin (14 mg/kg s.c.) in 1.5 mL two-thirds normal saline solution (40 mL/kg) for fluid resuscitation[8] at 6 hours after CLP. All animals were housed and sacrificed in accordance with the *National Institutional of Health Guide for the Care and Use of laboratory Animals* and with approval of the University of Arkansas for Medical Sciences Institutional Animal Care and Use Committee.

Measurements of Systemic Mean Arterial Blood Pressure and Heart Rate

Mean arterial pressure (MAP) and heart rate (HR) were measured in conscious mice using biotelemetry. Telemetry transmitters (Data Sciences International, Inc., St. Paul, MN) were implanted into the carotid artery of the mice under isoflurane anesthesia. After 4 days, mice were again anesthetized using isoflurane and underwent either CLP or sham surgery. At 6 hours after surgery, mice received antibiotic therapy and fluid resuscitation as described. Cardiovascular parameters were recorded every 5 minutes through 18 hours after CLP or sham surgery.

Renal Blood Flow

With the mice under isoflurane anesthesia, the right kidney was exposed using a flank incision, and the renal artery and vein were carefully dissected from surrounding tissue using Dumont No. 5 forceps. The renal artery was isolated from the vein, and a Doppler flow probe (0.5 PSL renal artery flow probe; Transonic Systems, Inc., Ithaca, NY) was positioned around the renal artery. The probe was calibrated in distilled water using the zero and scale setting of the TS420 flowmeter (Transonic Systems, Inc.). Body temperature was monitored using a rectal probe, and was maintained at 36°C to 37°C using a heating lamp. Blood flow readings were recorded using commercially available software (PowerLab and LabChart; ADInstruments, Ltd., Sydney, Australia) for 10 minutes after the flow had stabilized. Renal blood flow (RBF) was averaged over the 10-minute measurement period, and was expressed in milliliters per minute per gram kidney weigh (right kidney).

Glomerular Filtration Rate

Glomerular filtration rate (GFR) was measured using the single-bolus FITC-inulin clearance method.[19] In brief, mice were injected with a 5% FITC-inulin solution in normal saline vehicle at a dose of 3.74 μL/g via the tail vein. Blood (25 μL) was collected in heparinized capillary tubes at 3, 7, 10, 15, 35, 55, 75, 90, and 120 minutes after injection. FITC-inulin was measured at 485 nm excitation and 538 emission, and was quantified against a standard curve. Inulin clearance was calculated using a two-phase decay nonlinear regression analysis. GFR was calculated using the fast and slow phases of inulin clearance after normalizing to the combined weight of both kidneys, as described elsewhere.[19]

Serum Nitrate/Nitrite Concentrations

Serum nitrate/nitrite (NOx) concentrations, used as a marker of systemic NO generation, were determined using the Total Nitric Oxide Assay Kit (Assay Designs, Inc., Ann Arbor, MI) as directed by the manufacturer. In brief,

nitrate in serum samples was converted to nitrite using nitrate reductase. Data were expressed as serum NOx concentration in micromolar.

Intravital Videomicroscopy

Intravital videomicroscopy (IVVM) of the mouse kidneys was performed as previously described.[14,15,20,21] In brief, mice were anesthetized using isoflurane, and the left kidney was exposed via a flank incision. The kidney was positioned on a glass stage above an Axiovert 200 inverted fluorescence microscope equipped with an Axiocam HSm digitizing camera (both from Carl Zeiss AG, Jena, Germany) and kept moist using saline solution, and were covered. During the entire IVVM procedure, core temperature was monitored using a rectal temperature probe, and was maintained at 36°C to 37°C using an infrared heat lamp. At the end of IVVM, blood was collected from the inferior vena cava, and the mouse was sacrificed via cervical dislocation. The right kidney was fixed in 10% phosphate-buffered formalin.

Evaluation of Renal Peritubular Capillary Perfusion

At 10 minutes before IVVM, mice were administered FITC-dextran (500,000 Da, 2 μmol/kg) with DHR-123 (1.1 mg/kg) or MitoSOX (1.67 mg/kg) in a total volume of 3 mL/kg via the penile vein. During IVVM, the renal intravascular space and red blood cell movement were visualized with FITC-dextran using an excitation of 470 nm and an emission of 520 nm. For each mouse, five 10-second videos were captured at approximately 30 frames per second from five randomly selected fields of view. Capillary perfusion was analyzed as described previously.[14] In brief, approximately 150 randomly selected vessels per kidney were classified into three categories of blood perfusion: "continuous flow," in which red blood cell movement in the vessel was not interrupted during the video; "intermittent flow," in which red blood cell movement stopped or reversed at any time during the video; and "no flow," in which no red blood cell movement was detected. Data were expressed as the percentage of vessels in each of the three categories.

Evaluation of Renal Tubular Epithelial Cell RNS and Superoxide Generation Using IVVM

DHR-123 is oxidized to fluorescent rhodamine preferentially by the RNS peroxynitrite.[22] MitoSOX Red is a triphenylphosphonium derivative of dihydroethidine, which targets it to the mitochondria, where oxidation by superoxide and possibly other reactive oxygen species (ROS) yields a fluorescent product.[23] Rhodamine or MitoSOX fluorescence was visualized at 535 nm excitation and 590 nm emissions, and captured during IVVM from five randomly selected fields of view (×200 magnification) using a 500-msec exposure. Fluorescence intensity of each image was quantified using AxioVision Image Software (Carl Zeiss AG) after subtracting background fluorescence intensity. Data were expressed as arbitrary units per square micrometer.

Assay for Superoxide Scavenging Activity

The ability of MnTMPyP to scavenge superoxide was assessed by monitoring reduction of cytochrome *c* by superoxide generated from xanthine/xanthine oxidase as described elsewhere.[17] In brief, superoxide generation was initiated by adding xanthine oxidase (0.23 U/mL) to the reaction solution containing 50 mmol/L phosphate buffer (pH 7.8), 1 mmol/L EDTA, 40 μmol/L xanthine, and 11 μmol/L cytochrome *c*. After obtaining the initial rate of reduction of cytochrome *c* measured at 550 nm, MnTMPyP was added in varying concentrations. After the addition of MnTMPyP, the change in the rate of reduction of cytochrome *c* was determined. The data were expressed as percent inhibition of the initial rate of reduction of cytochrome *c* for each concentration of MnTMPyP. From these data, the IC_{50} value (half maximal inhibitory concentration) for MnTMPyP was calculated.

Evaluation of Renal Tubular Epithelial Redox Stress Using IVVM

NADPH autofluorescence was used as an indicator of cellular redox stress.[24,25] NADPH autofluorescence was visualized at 365 nm excitation and 420 nm emission, and captured from five randomly selected fields of view (×200) using a 500-msec exposure. Fluorescence intensity of each image was quantified using AxioVision Image Software (Carl Zeiss AG) after subtracting background fluorescence intensity. Data were expressed as arbitrary units per square micrometer.

Assessment of Renal Microvascular Permeability Using Evans Blue Dye

Renal microvascular permeability was assessed as described by Yasuda et al[26] with slight modifications. At 30 minutes before sacrifice, mice were injected with Evans Blue dye (1% in 0.9% saline solution) at 2 mL/kg via the tail vein. At sacrifice, mice were perfused using 30 mL PBS through the left ventricle until all blood was removed. The right kidney was weighed, homogenized in 1 mL formamide, and incubated at 55°C for 18 hours. The supernatant was collected after centrifugation at 12,000 × *g* for 30 minutes. The amount of Evans Blue dye in the supernatant was determined by measuring absorbance at 620 nm and correcting for turbidity at 740 nm, as described by Moitra et al[27] Evans Blue dye concentrations were determined from a standard curve and expressed as micrograms per gram kidney wet weight (right kidney).

Evaluation of Renal Tubular Hypoxia

Renal hypoxia was assessed using the Hypoxyprobe-1 Plus Kit (Natural Pharmacia International, Inc., Burlington, MA). The probe, pimonidazole (PIM), is reductively acti-

vated in low oxygen tension to a species that binds to cellular proteins.[28] Thus, immunoreactive adducts form in areas of low oxygen tension. PIM was administered at 60 mg/kg i.p. at 120 minutes before sacrifice. The left kidney was harvested and fixed in formalin for 24 hours. Fixed kidneys embedded in paraffin were cut into 5-μm sections and stained for PIM adducts. After rehydration, antigens were unmasked in 10 mmol/L sodium citrate (pH 6.0), heated to 95°C for 30 minutes, and allowed to cool. Slides were then blocked with serum-free protein block (Dako Corp., Carpinteria, CA), followed by addition of Hypoxyprobe-1 FITC-MAB1 antibody diluted 1:125, and incubated for 30 minutes at room temperature in a humid chamber. Peroxidase-conjugated anti-FITC secondary antibody diluted 1:125 was added, and the slides were incubated for 30 minutes at room temperature. A chromogen reagent supplied in the LSAB+ System–HRP Kit (Dako Corp.) was used to visualize antigen binding. Kidney sections were counterstained using Gill hematoxylin.

Nitrotyrosine Staining

Fixed kidneys embedded in paraffin were cut into 5-μm sections and stained for nitrotyrosine-protein adducts. After rehydration, antigens were unmasked in 10 mmol/L sodium citrate (pH 6.0), heated to 95°C for 30 minutes, and allowed to cool. Slides were then blocked with serum-free protein block (Dako Corp.), followed by addition of polyclonal anti-nitrotyrosine antibody (Millipore Corp., Billerica, MA) diluted 1:500. After overnight at 4°C in a humid chamber, slides were washed and incubated with secondary antibody from the LSAB+ System–HRP kit (Dako Corp.). A chromogen reagent supplied in the LSAB+ System–HRP Kit was used to visualize antigen binding. Nonspecific binding of the anti-nitrotyrosine antibody was determined by preincubating the antibody with 1 mmol/L 3-nitrotyrosine. Kidney sections were counterstained using Gill hematoxylin.

Serum Urea Nitrogen, Creatinine, and Alanine Aminotransferase

Blood urea nitrogen (BUN) and creatinine concentrations in serum were measured using the QuantiChrom Urea Assay Kit and the Creatinine Assay Kit, respectively (BioAssay Systems LLC, Hayward, CA). Alanine aminotransferase was measured using a Cobas Mira Clinical Analyzer (Roche Diagnostic Systems, Inc., Branchburg, NJ). Data were expressed as serum BUN and serum creatinine (SCr) concentrations in milligrams per deciliter, and serum alanine aminotransferase concentration in international units per liter.

Renal Tubular Injury Score

Paraffin-embedded sections (5 μm) were prepared from kidneys fixed in 10% phosphate-buffered formalin. PAS stain was used for analysis of tubular architecture, with light microscopy (Nikon E800; Nikon Instruments, Inc., Melville, NY). Sections were scored in a blinded semiquantitative manner using an established scoring scale.[29] For each animal, at least 10 high-power ($\times$400) fields were examined. The percentage of tubules that exhibited cellular necrosis, loss of brush border, cast formation, vacuolization, and tubule dilation were scored as follows: 0 = none, 1 = $<$10%, 2 = 11% to 25%, 3 = 26% to 45%, 4 = 46% to 75%, and 5 = $>$76%.

MnTMPyP Treatment

MnTMPyP, a cell membrane–permeable superoxide dismutase mimetic and peroxynitrite scavenger[17,18] was evaluated at a dose of 10 mg/kg in normal saline solution (0.9% NaCl i.p.). This dose was based on previous studies using MnTMPyP and other manganese porphyrins in rodents.[16,30,31] Mice were treated with MnTMPyP or saline solution immediately after CLP (0 hours) or at 6 hours after CLP.

Survival Study

Mice subjected to CLP were administered either MnTMPyP (10 mg/kg i.p.) or saline solution at 6 hours after CLP, and were monitored for 48 hours. Core body temperature was used as an indicator of pending death[32] and was measured every 6 hours using a rectal probe. Mice were considered nonsurvivors if they died or had to be euthanized because of two consecutive core temperature readings of less than 28°C.

Statistical Analysis

Data describing vessel flow were transformed using additive log-ratio transformations. Multivariate multiple regression analysis was used to evaluate changes in vessel composition as a function of time since CLP. The model included linear and quadratic functions of time to model the curvature present in the data. Similarly, multivariate analysis of variance models was used to evaluate vessel composition data for experiments investigating the effects of MnTMPyP on CLP. The Tukey-Kramer method was used to adjust for multiple comparisons. Hemodynamic data obtained at telemetry were analyzed using two-way analysis of variance. Other data with three or more groups were analyzed using one-way analysis of variance followed by the Newman-Keuls or Dunnett *post hoc* tests, with the exception of the renal tubular injury scores, which were analyzed using the nonparametric Kruskal-Wallis test followed by the Dunn multiple-comparisons test. Survival curve was analyzed using a Mantel-Cox log-rank test. Statistical significance was considered at $P < 0.05$.

Results

Hemodynamic Changes after CLP

To measure the systemic hemodynamic changes during sepsis in older C57BL mice subjected to CLP, we recorded MAP and HR in conscious mice using telemetry

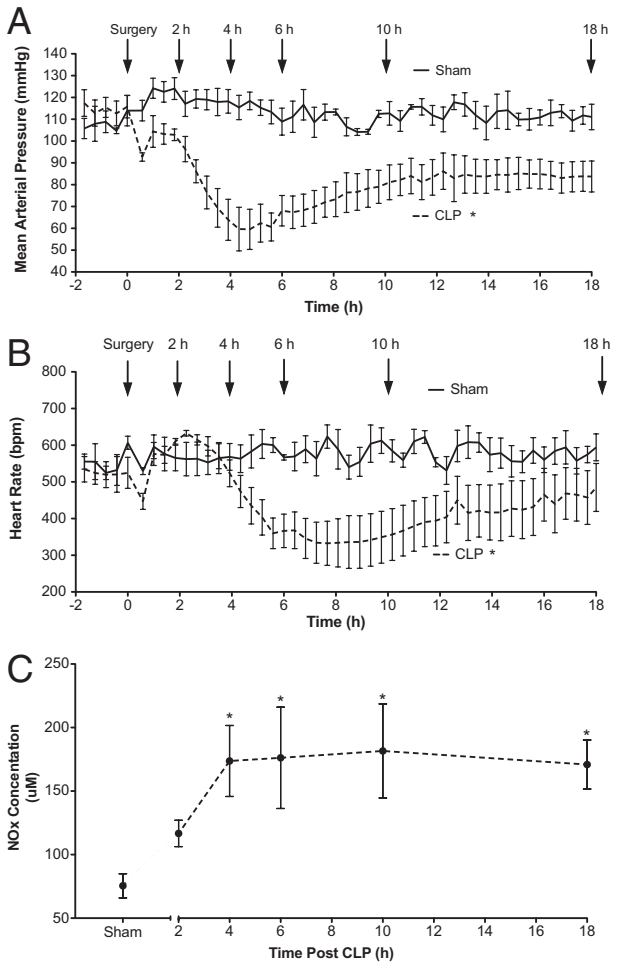

Figure 1. Systemic hemodynamic responses and serum nitrite/nitrate levels in mice after CLP. MAP (**A**) and HR (**B**) were recorded using biotelemetry after CLP or sham surgery. Fluids and antibiotics were administered at 6 hours after surgery (*Materials and Methods*). Data are given as mean ± SEM for 4 to 8 mice per group. $^*P < 0.05$ compared with Sham. **C:** Time course of change in serum NOx levels. Data are given as mean ± SEM for 5 to 11 mice per group. $^*P < 0.05$ compared with Sham.

(Figure 1, A and B, respectively). In Sham mice, MAP remained relatively stable at 100 to 120 mm Hg before and after sham surgery. In contrast, MAP in CLP mice was significantly lower compared with that in Sham mice. MAP declined rapidly during the first 6 hours to approximately 60 mm Hg, a value below the minimal renal autoregulatory pressure reported for the mouse.[33] MAP then slowly increased to approximately 85 mm Hg by 12 hours, and remained relatively stable through 18 hours. Like MAP, HR did not change in Sham mice. In CLP mice, HR decreased significantly compared with that in Sham mice; however, the decrease was delayed relative to the decrease in MAP.

Increased systemic NO synthesis accompanying hypotension is a feature of sepsis in humans.[34] The time course of serum NOx concentration in mice subjected to CLP is shown in Figure 1C. Because NOx concentrations in serum from Sham mice at 6 and 18 hours were not different, the value for Sham mice is from pooled data. NOx levels were significantly elevated at 4 hours after CLP compared with sham surgery, and were sustained through 18 hours.

Renal Capillary Dysfunction

The time course of changes in renal cortical capillary perfusion during sepsis was assessed using IVVM. Renal peritubular capillary perfusion declined rapidly after CLP (Figure 2A). The distribution of vessels with continuous, intermittent, and no flow changed over time, reaching significance by 4 hours, compared with the Sham control group (pooled data from 6 and 18 hours for Sham mice). Vessels with continuous flow decreased from 87% ± 3% in Sham mice to 53% ± 5% in CLP mice. This decline was accompanied by an increase in the percentage of vessels with no flow, from 7% ± 1% in Sham mice to 29% ± 4% in CLP mice. The impaired renal capillary perfusion was sustained through 18 hours.

RBF and GFR after CLP

The time course of changes in RBF during sepsis is shown in Figure 2B. RBF in CLP mice was not different from that in Sham mice (pooled data from 6 and 18 hours) at 2 hours, but was decreased significantly at 4, 6, and 18 hours. The decline in RBF paralleled the decline in systemic blood pressure and peritubular capillary perfusion. GFR also declined significantly at 6 and 18 hours after CLP compared with that in Sham mice (Figure 2B, inset).

Renal Vascular Permeability

Increased microvascular permeability and leakage is an important pathogenic feature of vascular dysfunction associated with sepsis-induced organ injury.[35] Using leakage of Evans Blue dye into the interstitial space as an indicator of increased permeability, CLP caused a significant 4-fold increase in permeability as early as 2 hours after CLP compared with sham operation (data from 6 hours in Sham mice) and a nearly 10-fold increase at 4 hours after CLP (Figure 2C). Thus, the increase in microvascular permeability preceded the decline in RBF and peritubular capillary perfusion, indicating that direct injury to the renal microvasculature occurred before renal hemodynamic failure.

Renal Tubular Epithelial Redox Stress and Hypoxia

The time course of NADPH autofluorescence, an indicator of cellular redox stress,[24,25] is shown in Figure 3A. Image analysis indicated that NADPH autofluorescence intensity was significantly increased at 4 hours after CLP compared with sham surgery (pooled data from 6 and 18 hours in Sham mice) and was sustained through 18 hours.

The severe decline in peritubular capillary perfusion suggested a decline in oxygen delivery. To assess renal tubular hypoxia, PIM-protein adducts were used

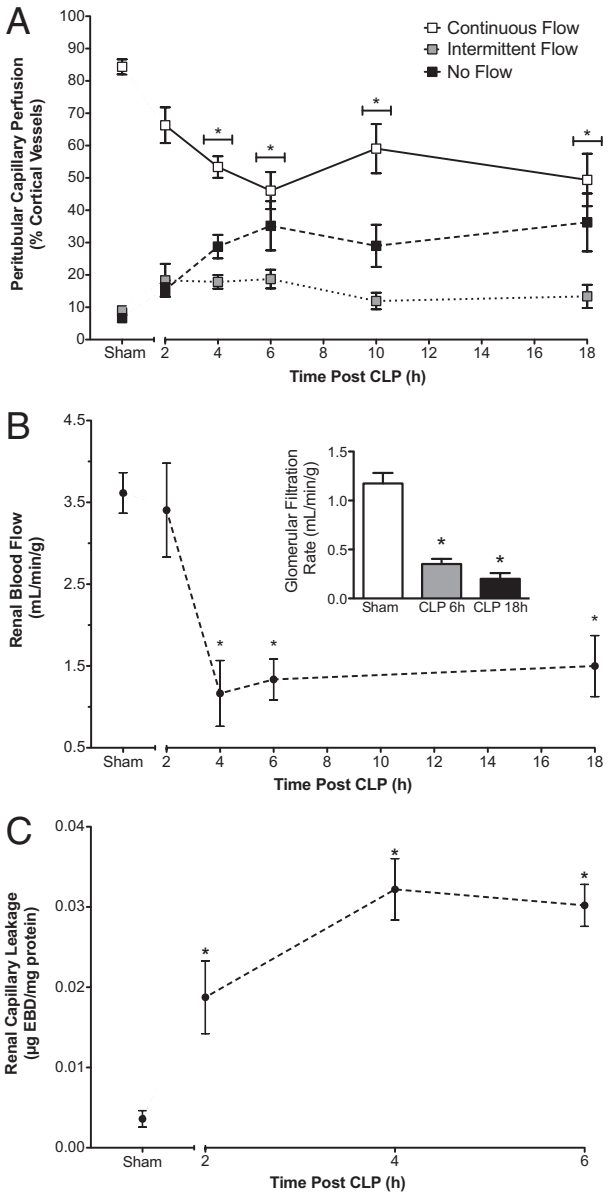

Figure 2. Effects of CLP on renal cortical peritubular capillary perfusion, RBF, and capillary leakage. **A:** Time-dependent changes in the distribution of cortical peritubular capillaries with continuous, intermittent, or no flow. CLP produced a significant decrease in the percentage of capillaries with continuous flow and an increase in the percentage of capillaries with no flow compared with Sham beginning at 4 hours. CLP also produced a rapid time-dependent decrease in RBF (**B**) and decreased GFR (**B**, **inset**). (**C**) Renal capillary permeability was assessed using Evans Blue dye (*Materials and Methods*). CLP caused a significant increase in Evans Blue dye leakage before the decline in capillary perfusion and RBF. Data are given as mean ± SEM for 6 to 11 mice per group (**A**), 5 to 11 mice per group (**B**), 4 mice per group (**B**, **inset**), and 4 or 5 mice per group (**C**). $^*P < 0.05$ compared with Sham.

as a marker of low oxygen tension.[33] Representative images of PIM-protein adducts are shown in Figure 3B. Few adducts were detected in Sham mouse kidneys, whereas adducts were clearly visible in the tubules of the cortex and cortico-medullary junction with little staining in glomeruli as early as 4 hours after CLP, and the amount of adducts appeared to increase by 6 hours.

ROS and RNS Generation by Renal Tubular Cells after CLP

Oxidation of mitochondria-targeted MitoSOX[23] by superoxide and other ROS was used to quantify ROS generation using IVVM. Image analysis demonstrated a time-dependent increase in MitoSOX oxidation (Figure 4A), which reached significance compared with Sham mice (pooled data from 6 and 18 hours) at 4 hours. Representative images of the same field of view for FITC-dextran (capillary perfusion) and MitoSOX are shown in Figure 4, B and C, respectively. MitoSOX fluorescence was generally localized to tubules bordered by capillaries with no flow.

Superoxide reacts with NO to generate the RNS peroxynitrite,[36] which nitrates protein and oxidizes dihydrorhodamine to fluorescent rhodamine. Representative immunohistochemical images for nitrotyrosine-protein adducts in Sham and CLP mice at 6 and 18 hours are shown in Figure 5A. At 6 hours after CLP, nitrotyrosine-protein adducts were clearly evident in tubules in the cortex. Adducts appeared to increase further by 18 hours. Staining in Sham mouse kidneys was not different from the nonspecific staining control (data not shown). Representative images captured during IVVM of the same field of view for FITC-dextran and rhodamine are shown in Figure 5B. As with MitoSOX fluorescence, rhodamine fluorescence was generally localized to tubules bordered by capillaries with no flow. Using image analysis to quantify rhodamine fluorescence, we observed significantly increased fluorescence density, which suggested RNS generation at 6 and 18 hours after CLP compared with sham surgery (Figure 5C).

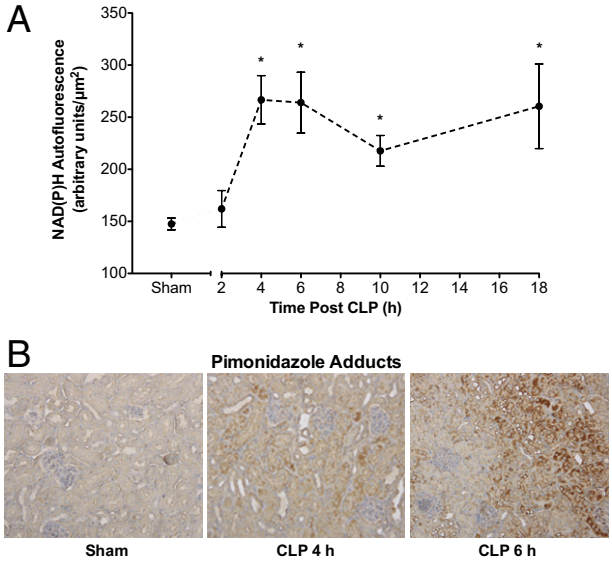

Figure 3. Time course of CLP-induced changes in renal NADPH levels and PIM protein-adduct formation. **A:** Tubular NADPH levels were assessed using IVVM. CLP produced a significant time-dependent increase in NADPH levels beginning at 4 hours after CLP. Data are given as mean ± SEM for 6 to 11 mice per group. $^*P < 0.05$ compared with Sham. **B:** Representative images (×200) from 3 or 4 mice per group of PIM-protein adducts. No specific staining for PIM-protein adducts was apparent in Sham mice (6 hours after surgery). Staining (brown) was visible at 4 hours after CLP, and was patchy in the cortex. At 6 hours after CLP, staining was more intense and more widespread throughout the cortex.

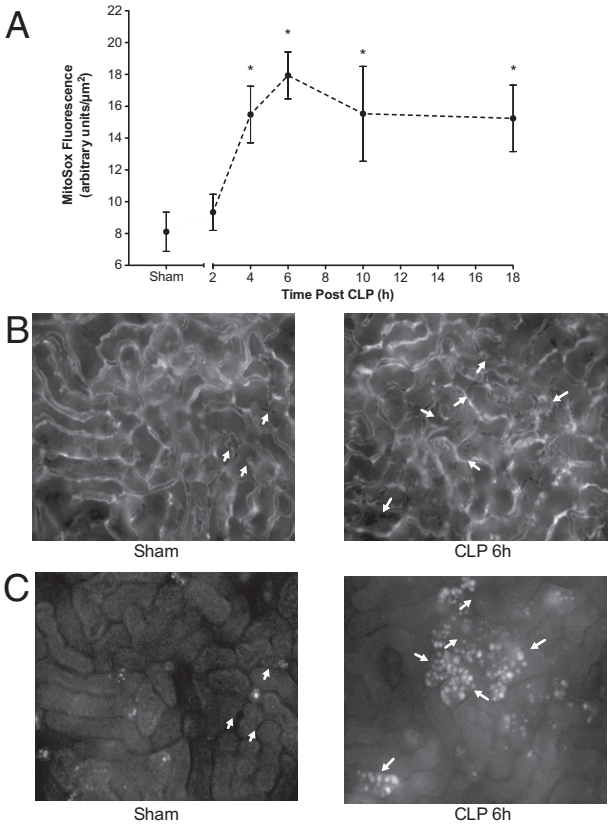

Figure 4. Time course of CLP-induced changes in cortical MitoSOX oxidation. MitoSOX oxidation, an indicator of ROS generation, was assessed using IVVM. **A:** Time course of the increase in MitoSOX fluorescence. CLP produced a significant increase in MitoSOX fluorescence beginning at 4 hours after CLP. Data are given as mean ± SEM for 4 to 7 mice per group. $^*P < 0.05$ compared with Sham. **B:** Representative images from videos (×200) of 4 to 6 mice per group of FITC-dextran to visualize the capillary vascular space. Red blood cells are observed as shadows in the white capillary spaces. **Arrows** indicate capillaries with no flow. **C:** Images of MitoSOX fluorescence in the same fields of view as in **B** to compare the relationships between capillary perfusion and MitoSOX fluorescence.

Delayed Treatment with MnTMPyP Restores Peritubular Capillary Perfusion and Reduces ROS/RNS Generation and Cellular Redox Stress

We first confirmed that MnTMPyP tetratosylate hydroxide was an effective scavenger of superoxide by testing it against xanthine oxidase–generated superoxide. MnTMPyP produced a concentration-dependent scavenging of superoxide with an IC_{50} of 1.18 μmol/L (95% CI, 0.68–2.04 μmol/L). To evaluate the therapeutic potential of MnTMPyP, a single dose (10 mg/kg i.p.) was administered after the onset of sepsis because sepsis typically is treated only after the onset of symptoms. We chose to treat at 6 hours after CLP because this was the time of greatest decline in renal capillary perfusion and the peak of ROS generation in the cortical tubules. At 18 hours, MnTMPyP had no effect on cortical peritubular capillary perfusion in Sham mice but reversed the decline in perfusion in CLP mice (Figure 6A). Delayed treatment with MnTMPyP also significantly reduced NADPH autofluorescence (Figure 6B), MitoSOX fluorescence (Figure 6C), and nitrotyrosine-protein adducts (Figure 6D) at 18 hours, and inhibited rhodamine fluorescence by 89% ± 24% when compared with CLP alone ($n = 3$ to 6; $P < 0.05$). In contrast, MnTMPyP did not reduce systemic NO generation [171 ± 19 μmol/L for CLP versus 151 ± 26 μmol/L for CLP plus MnTMPyP administered at 6 hours ($n = 6$; $P > 0.05$)], indicating that MnTMPyP acted downstream of NO synthesis.

Effects of Delayed Treatment with MnTMPyP on Hemodynamics, Renal Function, and Tubular Architecture

The effect of MnTMPyP administered at 6 hours after surgery (10 mg/kg i.p.) on MAP and HR are shown in Figure 7, A and B, along with Sham and CLP control data redrawn from Figure 1, A and B, for reference. MnTMPyP produced a slight but significant increase in MAP in Sham mice but did not change MAP in CLP mice. In contrast, MnTMPyP produced a slight but significant increase in HR in both Sham and CLP mice. These data suggest that the effects of MnTMPyP on renal capillary perfusion were not due to changes in MAP.

MnTMPyP did not alter SCr or BUN levels in Sham mice at 18 hours (data not show). At 18 hours after CLP, SCr (Figure 7C) and BUN (Figure 7D) concentrations were both significantly elevated compared with those in Sham mice at 18 hours. Delayed treatment with MnTMPyP significantly reduced both SCr and BUN concentrations; however, the increase in BUN was not completely blocked. Inasmuch as SCr is not a reliable indicator of GRF in mice

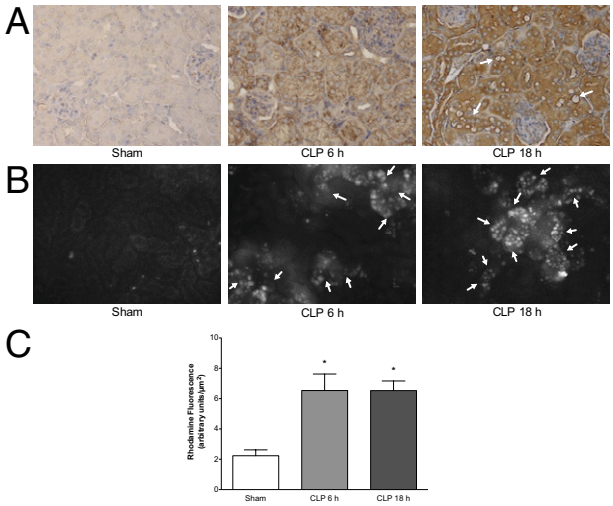

Figure 5. CLP-induced RNS generation in the kidney cortex. **A:** Representative images from 4 mice per group of the immunohistochemical staining for nitrotyrosine-protein adducts. Staining in Sham-operated mouse kidneys was not different from nonspecific staining (pre-incubation of the primary antibody with 10 mmol/L 3-nitrotyrosine; image not shown). Nitrotyrosine-protein adducts (×200; brown) were visible in the cortex but not the glomeruli at 6 hours after CLP. At 18 hours after CLP, nitrotyrosine-protein adducts were widespread and clearly visible around tubules with morphologic damage. **Arrows** indicate tubules with vacuolization. **B:** Representative images of rhodamine fluorescence (oxidized DHR-123). **Arrows** indicate capillaries with no flow identified via analysis of videos with FITC-dextran in the same fields of view to compare the relationships between capillary perfusion and RNS generation. **C:** Image analysis showed a significant increase in rhodamine fluorescence at 6 and 18 hours compared with Sham. Data are given as mean ± SEM for 6 to 9 mice per group. $^*P < 0.05$.

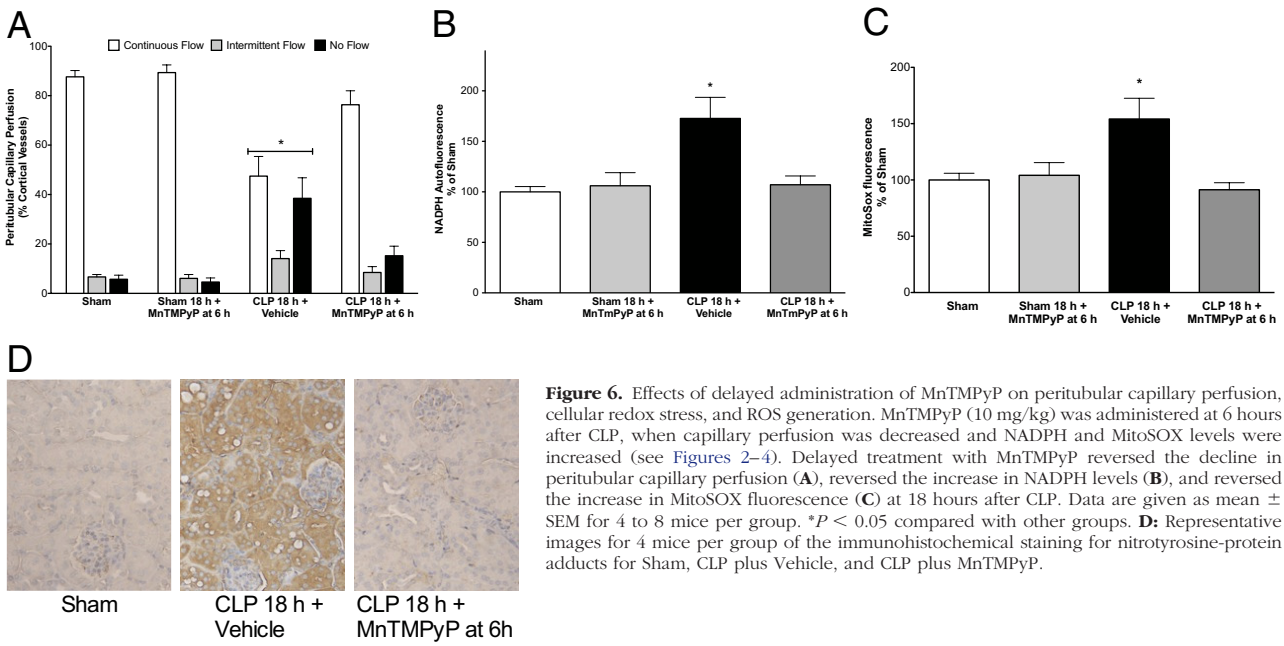

Figure 6. Effects of delayed administration of MnTMPyP on peritubular capillary perfusion, cellular redox stress, and ROS generation. MnTMPyP (10 mg/kg) was administered at 6 hours after CLP, when capillary perfusion was decreased and NADPH and MitoSOX levels were increased (see Figures 2–4). Delayed treatment with MnTMPyP reversed the decline in peritubular capillary perfusion (**A**), reversed the increase in NADPH levels (**B**), and reversed the increase in MitoSOX fluorescence (**C**) at 18 hours after CLP. Data are given as mean ± SEM for 4 to 8 mice per group. $^*P < 0.05$ compared with other groups. **D:** Representative images for 4 mice per group of the immunohistochemical staining for nitrotyrosine-protein adducts for Sham, CLP plus Vehicle, and CLP plus MnTMPyP.

with sepsis,[37] GFR was measured using inulin clearance.[19] Delayed treatment with MnTMPyP partially but significantly restored GFR (Figure 7E) and completely restored RBF (Figure 7F). Representative images of PAS-stained cortical sections for Sham 18 hours plus MnTMPyP, CLP 18 hours, and CLP 18 hours plus MnTMPyP administered at 6 hours are shown in Figure 7, G–I, respectively. The CLP 18-hour group exhibited relatively mild morphologic renal damage characterized by mild brush border loss, tubular degeneration, and vacuolization in the early segments of proximal tubules, as reported by us[14,20] and by others.[8] Delayed treatment with MnTMPyP significantly reduced the morphologic injury score (Figure 7J).

Serum alanine aminotransferase concentration, a marker of liver injury, in Sham, CLP, and CLP plus MnTMPyP mice were 21 ± 5, 85 ± 16, and 33 ± 6 IU/L, respectively ($n = 6$ or 7; $P < 0.05$ for CLP mice compared with Sham and CLP plus MnTMPyP mice), indicating very mild hepatotoxicity, which was also blocked by MnTMPyP.

Effects of Delayed Administration of MnTMPyP on Survival

The ability of MnTMPyP to improve renal microcirculation and restore renal function led us to investigate the potential of MnTMPyP to increase survival. Based on the reported organ half-life for other metalloporphyrins in rodents of 60 to 135 hours,[38] CLP mice were given a single dose of MnTMPyP (10 mg/kg i.p.) at 6 hours, and were monitored through 48 hours (Figure 7K). Compared with untreated CLP mice, MnTMPyP significantly prolonged survival ($P < 0.01$, Mantel-Cox log-rank test).

Effects of MnTMPyP on Initial Renal Injury

To assess its effects on the initial renal injury, MnTMPyP (10 mg/kg i.p.) was administered at CLP. MnTMPyP significantly blocked MitoSOX fluorescence at 6 hours after CLP, confirming that the dose was effective in scavenging ROS (Figure 8A). However, MnTMPyP failed to prevent the initial declines in peritubular capillary perfusion (Figure 8B) and RBF (Figure 8C) or the increase in capillary leakage (Figure 8D).

Discussion

The hemodynamic changes associated with sepsis include progressive cardiovascular failure characterized by systemic vasodilation, inadequate microvascular perfusion, and impairment of tissue oxygenation. While no current animal models fully replicate all of the complexities of human sepsis, the CLP model in aged mice mimics some key features of severe septic shock in humans including release of cytokines with a similar magnitude and kinetic profile,[8,39] a decrease in MAP-associated increased systemic NO production[40] that is largely dependent on up-regulation of inducible NO synthase,[14,34] and similar renal tubular damage and decreased renal function, which occur relatively rapidly and progress to AKI.[2,34,41] Still, a limitation of this model is that it does not replicate the initial hyperdynamic circulation observed in sepsis.[42] Although this model of sepsis-induced AKI has been used for a number of years,[8] a detailed investigation of the changes in RBF, GFR, and peritubular capillary perfusion during the course of sepsis has never been performed.

We observed that RBF declined rapidly and dramatically after CLP, paralleling the decrease in MAP. This is in contrast to what is observed in the sheep after *Escherichia coli* infusion, where RBF increases over time[43,44]; however, in pigs subjected to autologous fecal peritonitis, a model more closely resembling CLP, RBF decreases slowly as MAP is reduced.[45,46] Because RBF in patients with sepsis is rarely measured, the relationships between MAP, RBF, and de-

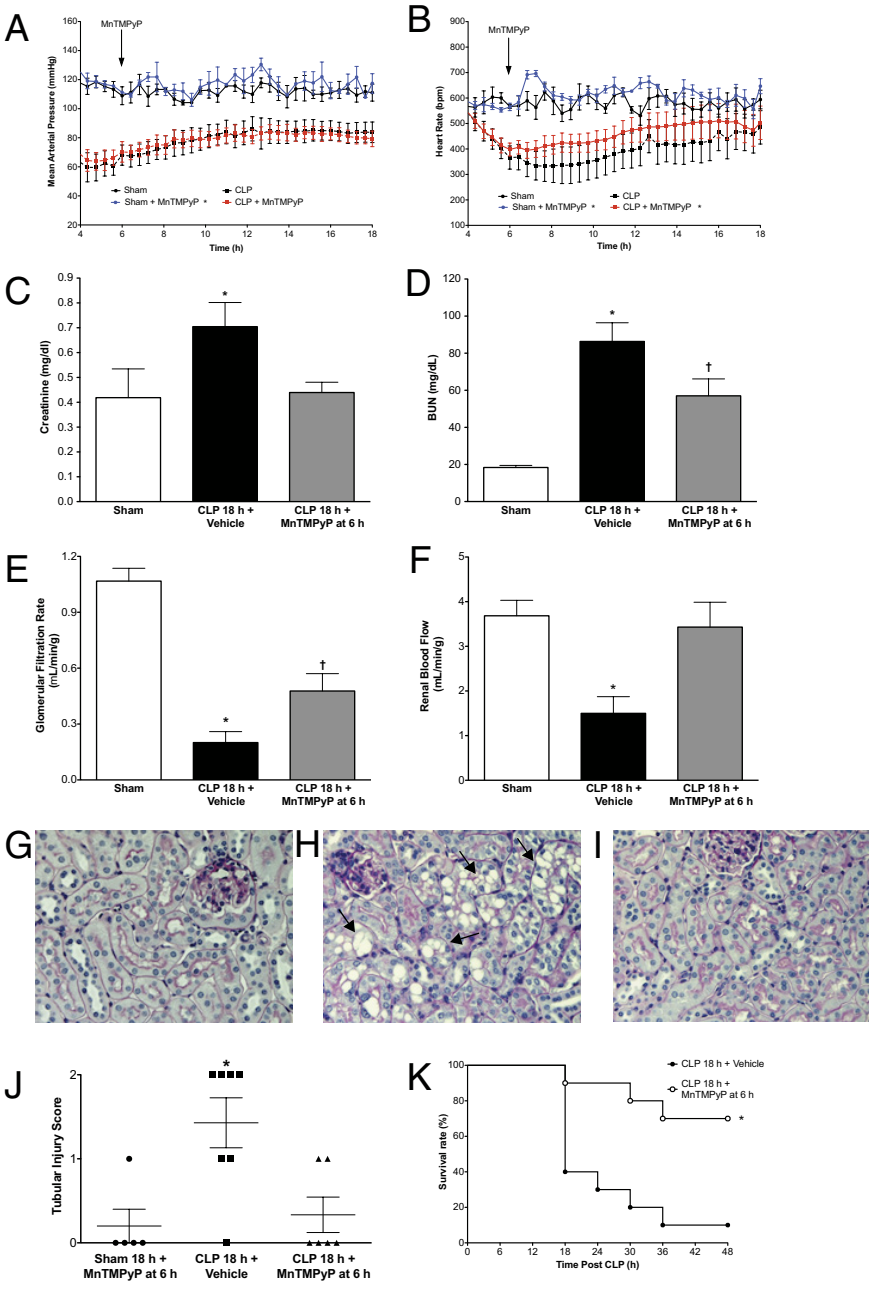

Figure 7. Effects of MnTMPyP on hemodynamics, renal function, tubular architecture, and survival. MnTMPyP (10 mg/kg) administered at 6 hours after CLP, when GRF and RBF were decreased (see Figure 2). MAP (**A**) and HR (**B**) for mice treated with MnTMPyP are shown, along with Sham and CLP control data replotted from Figure 1. MAP was increased in Sham plus MnTMPyP mice (*P < 0.05 compared with Sham) but not in CLP plus MnTMPyP mice, whereas HR was increased in both Sham plus MnTMPyP and CLP plus MnTMPyP mice (*P < 0.05 compared with Sham and CLP, respectively). Data are given as mean ± SEM for 4 to 6 mice per group. Delayed treatment with MnTMPyP prevented the increase in SCr concentration (**C**) and partially but significantly reduced serum BUN concentration (**D**). MnTMPyP also reversed the decline in GFR (**E**) and RBF (**F**). Data are given as mean ± SEM for 4 to 8 mice per group; *P < 0.05 compared with Sham, †P < 0.05 compared with Sham, and CLP 18 hours plus Vehicle. Representative images (×200) from 5 to 7 mice per group of PAS-stained cortex are shown for Sham (**G**), CLP 18 hours plus Vehicle (**H**), and CLP 18 hours plus MnTMPyP (**I**) mice treated at 6 hours. **Arrows** indicate representative tubules with vacuolization. **J:** Delayed treatment with MnTMPyP also reduced the tubular injury score. Data are plotted as individual scores with mean and range, and were analyzed using the Kruskal-Wallis test (*P < 0.05 compared with Sham). **K:** Administration of MnTMPyP in CLP mice at 6 hours resulted in a significant improvement in survival compared with that in untreated CLP control mice (*P < 0.01, Mantel-Cox log-rank test; n = 10 mice per group).

velopment of AKI in these critically ill patients are unknown. In the few patients in whom RBF has been measured, high variability in RBF among patients prevents reliable conclusions about the state of RBF during the course of sepsis-induced AKI.[47,48]

An important finding was how quickly renal capillaries became damaged, likely as a result of cytokine-mediated endothelial injury.[49] Evidence of renal capillary leakage after CLP in the mouse was first reported at 6 hours (the earliest time point measured) by Yasuda et al[26] Our data demonstrate that capillary leakage occurs as early as 2 hours after CLP, just preceding the decline in RBF and peritubular capillary perfusion. Whereas capillary leakage can contribute to reduced capillary perfusion,[49] decreased systemic MAP and increased renal vascular resistance more likely have a greater effect on RBF,[50] in particular because MAP decreased to below the reported autoregulatory pressure necessary to maintain GFR in the mouse.[33] Regardless of the cause, this combination of events was associated with development of a hypoxic pro-oxidant peritubular microenvironment and a decrease in GFR within 6 hours. The rapid decline in peritubular capillary perfusion coincided with development of localized areas of redox stress and hypoxia. Tubular generation of ROS was also temporally and spatially related to the decline in capillary perfusion, as was generation of peroxynitrite (the product of NO and superoxide) in the peritubular microenvironment. At 18 hours after CLP, the RBF, peritubular capillary perfusion, and GFR were still decreased despite a partial increase in MAP to above the

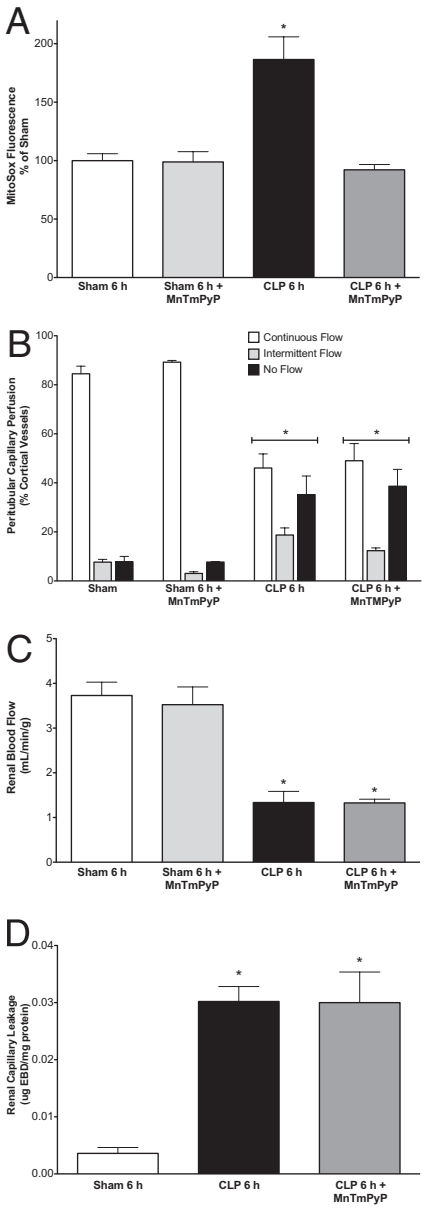

Figure 8. Effects of MnTMPyP on the early renal effects of CLP. MnTMPyP (10 mg/kg) administered at CLP blocked MitoSOX fluorescence at 6 hours (**A**), but did not alter the decline in peritubular capillary perfusion (**B**), RBF (**C**), or Evans Blue dye leakage (**D**). Data are given as mean ± SEM for 4 to 6 mice per group. $^*P < 0.05$ compared with Sham.

renal autoregulatory pressure, which suggests that the sustained oxidant generation and tubular damage contributed to the sustained renal hemodynamic failure as noted in renal ischemic injury.[51]

CLP-induced AKI is not due to hemodynamic failure alone (pre–renal AKI), which supports the emerging view that renal microcirculatory failure and direct tubular injury, even after correction of systemic hemodynamics, contribute significantly to sepsis-induced AKI in humans.[42] Targeting the early hemodynamic failure with the objective of maintaining organ perfusion[4] is not always effective in preserving organ function because the effects of the initial hemodynamic insult may be difficult to prevent or reverse.[52] Our data support the rationale for also targeting oxidant generation in the peritubular microenvironment[10] because ROS and RNS generation by the tubular epithelium are relatively later events clearly linked to tubular injury. ROS and RNS can activate extracellular matrix degrading enzymes,[20,53] damage cellular membranes,[36] and inhibit mitochondrial function.[54] These time course studies suggest a rapid transition from the initial capillary endothelial injury and renal hypoperfusion to a predominantly oxidative stress–mediated tubular injury, which then helps sustain the decline in renal capillary perfusion and renal function. A major finding of these studies is that scavenging ROS and RNS, even if delayed, reverses the decline in capillary perfusion and renal function.

Studies with the superoxide dismutase mimetic/peroxynitrite scavenger MnTMPyP[17,18] revealed mechanistic insights into early renal hemodynamic failure. Superoxide and perhaps peroxynitrite mediate, at least in part, the renal vasoconstrictor responses to endothelin and angiotensin II[55–57] and the loss in vasoreactivity in mesenteric microvessels from mice with sepsis.[58] We observed that MnTMPyP was unable to prevent renal capillary leakage and failed to preserve RBF or peritubular capillary perfusion during the first 6 hours after CLP despite reducing ROS levels, which suggests that these early renal hemodynamic defects are not superoxide- or peroxynitrite-dependent. Nevertheless, MnTMPyP was able to prevent tubular injury and actually reverse peritubular capillary hypoperfusion at 18 hours even when administered after the onset of renal hypoperfusion. This important finding supports the notion that preventing tubular injury may enable capillary perfusion to recover.[14,15,59] The mechanism of recovery of the microcirculation is unclear, but was not due to an increase in MAP because MnTMPyP did not alter MAP in CLP mice despite slightly increasing HR. The reason for this may be related to a potential increase in the bioavailability of NO in resistance vessels when superoxide levels are reduced.[58] Recovery of the renal microcirculation was likely due to the protection against oxidant-induced tubular epithelial injury. As tubular swelling, cell sloughing, and membrane damage occur, peritubular capillary perfusion is likely impeded further. This would augment local hypoxia[26] and oxidant generation to exacerbate tubular injury and capillary dysfunction.[15] Thus, MnTMPyP was able to break the cycle of injury by protecting the tubular epithelium and enabling recovery of capillary perfusion, RBF, and renal function. Moreover, a single dose of MnTMPyP administered at 6 hours after CLP dramatically improved 48-hour survival. Other metalloporphyrins likely share these protective effects because pretreatment with MnTE-2-PyP prevented the decline in RBF and GFR and also improved survival in a lipopolysaccharide model of sepsis.[16] Growing evidence suggests that preserving renal function during sepsis could reduce development of multiple-organ failure and death.[60] However, it is unlikely that MnTMPyP acted only in the kidney. Inasmuch as oxidative stress can occur in multiple organs during sepsis,[10,61] MnTMPyP may have had direct protective effects on other organs as well.

While the intracellular sources of ROS and RNS could not be identified in these studies, the protective effects of

MnTMPyP suggest that mitochondrial oxidant generation is at least one likely source[10] because MitoSOX is targeted to mitochondria[23] and MnTMPyP blocked the intracellular localization of both MitoSOX and rhodamine fluorescence in tubules. Moreover, MnTMPyP protects tubular epithelial mitochondria during renal ischemia and reperfusion.[62] Establishing the relative contributions of ROS and RNS to renal injury will require absolutely selective ROS and RNS scavengers, which are not yet available. Nevertheless, the protective effects of inducible NO synthase inhibitors in experimental models of sepsis also support the notion that RNS generation is critical to development of sepsis-induced AKI.[1,14,15,59]

Another striking finding was the very early decline in GRF, which persisted through 18 hours. Using inulin clearance,[19] we were able to detect a dramatic decline in GRF at 6 hours, which is earlier than previously thought based on SCr concentrations,[8,14] now regarded as a poor marker of renal function in sepsis due to reduced production of creatinine by mice with sepsis.[37] Although MnTMPyP at the dose used only partially restored GFR, the RBF and cortical peritubular capillary perfusion were restored and tubular architecture was preserved. Thus, oxidant generation in the peritubular microenvironment can be added to the growing list of drug targets amenable to delayed therapy in rodent models of sepsis-induced AKI[8,20,63–65] and provide proof-of-principle that superoxide dismutase mimetics and peroxynitrite scavengers should be evaluated further as possible therapeutic agents because targeting the later oxidant-damaging effects in the microcirculation could have a high likelihood of success in patients with sepsis.

Acknowledgments

We thank Dr. Shi Liu and Kerrey Roberto [University of Arkansas for Medical Sciences (UAMS) Rodent Biotelemetry Core] for assistance with the biotelemetry studies and the UAMS Experimental Pathology Core for tissue processing and histologic analysis.

References

1. Heemskerk S, Masereeuw R, Russel FG, Pickkers P: Selective iNOS inhibition for the treatment of sepsis-induced AKI. Nat Rev Nephrol 2009, 5:629–640
2. Bagshaw SM, Lapinsky S, Dial S, Arabi Y, Dodek P, Wood G, Ellis P, Guzman J, Marshall J, Parrillo JE, Skrobik Y, Kumar A: Acute kidney injury in septic shock: clinical outcomes and impact of duration of hypotension prior to initiation of antimicrobial therapy. Intensive Care Med 2009, 35:871–881
3. Ricci Z, Polito A, Ronco C: The implications and management of septic acute kidney injury. Nat Rev Nephrol 2011, 7:218–225
4. Levy MM, Dellinger RP, Townsend SR, Linde-Zwirble WT, Marshall JC, Bion J, Schorr C, Artigas A, Ramsay G, Beale R, Parker MM, Gerlach H, Reinhart K, Silva E, Harvey M, Regan S, Angus DC: The Surviving Sepsis Campaign: results of an international guideline-based performance improvement program targeting severe sepsis. Crit Care Med 2010, 38:367–374
5. Sakr Y, Dubois MJ, De Backer D, Creteur J, Vincent JL: Persistent microcirculatory alterations are associated with organ failure and death in patients with septic shock. Crit Care Med 2004, 32:1825–1831
6. Vincent JL, De Backer D: Microvascular dysfunction as a cause of organ dysfunction in severe sepsis. Crit Care 2005, 9(Suppl 4):S9–S12
7. Dudley C: Maximizing renal preservation in acute renal failure. BJU Int 2004, 94:1202–1206
8. Miyaji T, Hu X, Yuen PS, Muramatsu Y, Iyer S, Hewitt SM, Star RA: Ethyl pyruvate decreases sepsis-induced acute renal failure and multiple organ damage in aged mice. Kidney Int 2003, 64:1620–1631
9. Crouser ED: Mitochondrial dysfunction in septic shock and multiple organ dysfunction syndrome. Mitochondrion 2004, 4:729–741
10. Galley HF: Bench-to-bedside review: targeting antioxidants to mitochondria in sepsis. Crit Care 2010, 14:230
11. Brealey D, Brand M, Hargreaves I, Heales S, Land J, Smolenski R, Davies NA, Cooper CE, Singer M: Association between mitochondrial dysfunction and severity and outcome of septic shock. Lancet 2002, 360:219–223
12. Goode HF, Cowley HC, Walker BE, Howdle PD, Webster NR: Decreased antioxidant status and increased lipid peroxidation in patients with septic shock and secondary organ dysfunction. Crit Care Med 1995, 23:646–651
13. Spanos A, Jhanji S, Vivian-Smith A, Harris T, Pearse RM: Early microvascular changes in sepsis and severe sepsis. Shock 2010, 33:387–391
14. Wu L, Gokden N, Mayeux PR: Evidence for the role of reactive nitrogen species in polymicrobial sepsis-induced renal peritubular capillary dysfunction and tubular injury. J Am Soc Nephrol 2007, 18:1807–1815
15. Wu L, Mayeux PR: Effects of the inducible nitric oxide synthase inhibitor L-N6-(1-iminoethyl)-lysine on microcirculation and reactive nitrogen species generation in the kidney following lipopolysaccharide administration in mice. J Pharmacol Exp Ther 2007, 320:1061–1067
16. Wang W, Jittikanont S, Falk SA, Li P, Feng L, Gengaro PE, Poole BD, Bowler RP, Day BJ, Crapo JD, Schrier RW: Interaction among nitric oxide, reactive oxygen species, and antioxidants during endotoxemia-related acute renal failure. Am J Physiol Renal Physiol 2003, 284:F532–F537
17. Faulkner KM, Liochev SI, Fridovich I: Stable Mn(III) porphyrins mimic superoxide dismutase in vitro and substitute for it in vivo. J Biol Chem 1994, 269:23471–23476
18. Crow JP: Peroxynitrite scavenging by metalloporphyrins and thiolates. Free Rad Biol Med 2000, 28:1487–1494
19. Qi Z, Whitt I, Mehta A, Jin J, Zhao M, Harris RC, Fogo AB, Breyer MD: Serial determination of glomerular filtration rate in conscious mice using FITC-inulin clearance. Am J Physiol Renal Physiol 2004, 286: F590–F596
20. Wang Z, Herzog C, Kaushal GP, Gokden N, Mayeux PR: Actinonin, a meprin A inhibitor, protects the renal microcirculation during sepsis. Shock 2011, 35:141–147
21. Wu L, Tiwari MM, Messer KJ, Holthoff JH, Gokden N, Brock RW, Mayeux PR: Peritubular capillary dysfunction and renal tubular epithelial cell stress following lipopolysaccharide administration in mice. Am J Physiol Renal Physiol 2007, 292:F261–F268
22. Gomes A, Fernandes E, Lima JL: Use of fluorescence probes for detection of reactive nitrogen species: a review. J Fluoresc 2006, 16:119–139
23. Robinson KM, Janes MS, Pehar M, Monette JS, Ross MF, Hagen TM, Murphy MP, Beckman JS: Selective fluorescent imaging of superoxide in vivo using ethidium-based probes. Proc Natl Acad Sci USA 2006, 103:15038–15043
24. Paxian M, Keller SA, Cross B, Huynh TT, Clemens MG: High-resolution visualization of oxygen distribution in the liver in vivo. Am J Physiol Gastrointest Liver Physiol 2004, 286:G37–G44
25. Wunder C, Brock RW, Krug A, Roewer N, Eichelbronner O: A remission spectroscopy system for in vivo monitoring of hemoglobin oxygen saturation in murine hepatic sinusoids, in early systemic inflammation. Comp Hepatol 2005, 4:1(online), doi:10.1186/1476-5926-4-1
26. Yasuda H, Yuen PS, Hu X, Zhou H, Star RA: Simvastatin improves sepsis-induced mortality and acute kidney injury via renal vascular effects. Kidney Int 2006, 69:1535–1542
27. Moitra J, Sammani S, Garcia JG: Re-evaluation of Evans Blue dye as a marker of albumin clearance in murine models of acute lung injury. Trans Res 2007, 150:253–265
28. Arteel GE, Thurman RG, Raleigh JA: Reductive metabolism of the hypoxia marker pimonidazole is regulated by oxygen tension inde-

pendent of the pyridine nucleotide redox state. Eur J Biochem 1998, 253:743–750
29. Wang W, Faubel S, Ljubanovic D, Mitra A, Kim J, Tao Y, Soloviev A, Reznikov LL, Dinarello CA, Schrier RW, Edelstein CL: Endotoxemic acute renal failure (ARF) is attenuated in caspase-1 deficient mice. Am J Physiol Renal Physiol 2005, 288:F997–F1004
30. Mortensen J, Shames B, Johnson CP, Nilakantan V: MnTMPyP, a superoxide dismutase/catalase mimetic, decreases inflammatory indices in ischemic acute kidney injury. Inflamm Res 2011, 60:299–307
31. Nin N, Cassina A, Boggia J, Alfonso E, Botti H, Peluffo G, Trostchansky A, Batthyany C, Radi R, Rubbo H, Hurtado FJ: Septic diaphragmatic dysfunction is prevented by Mn(III)porphyrin therapy and inducible nitric oxide synthase inhibition. Intensive Care Med 2004, 30:2271–2278
32. Warn PA, Brampton MW, Sharp A, Morrissey G, Steel N, Denning DW, Priest T: Infrared body temperature measurement of mice as an early predictor of death in experimental fungal infections. Lab Anim 2003, 37:126–131
33. Vallon V, Traynor T, Barajas L, Huang YG, Briggs JP, Schnermann J: Feedback control of glomerular vascular tone in neuronal nitric oxide synthase knockout mice. J Am Soc Nephrol 2001, 12:1599–1606
34. Heemskerk S, Pickkers P, Bouw MP, Draisma A, van der Hoeven JG, Peters WH, Smits P, Russel FG, Masereeuw R: Upregulation of renal inducible nitric oxide synthase during human endotoxemia and sepsis is associated with proximal tubule injury. Clin J Am Soc Nephrol 2006, 1:853–862
35. Kumar P, Shen Q, Pivetti CD, Lee ES, Wu MH, Yuan SY: Molecular mechanisms of endothelial hyperpermeability: implications in inflammation. Expert Rev Mol Med 2009, 11:e19
36. Beckman JS: Oxidative damage and tyrosine nitration from peroxynitrite. Chem Res Tox 1996, 9:836–844
37. Doi K, Yuen PS, Eisner C, Hu X, Leelahavanichkul A, Schnermann J, Star RA: Reduced production of creatinine limits its use as marker of kidney injury in sepsis. J Am Soc Nephrol 2009, 20:1217–1221
38. Batinic-Haberle I, Reboucas JS, Spasojevic I: Superoxide dismutase mimics: chemistry, pharmacology, and therapeutic potential. Antioxid Redox Signal 2010, 13:877–918
39. Doi K, Leelahavanichkul A, Yuen PS, Star RA: Animal models of sepsis and sepsis-induced kidney injury. J Clin Invest 2009, 119: 2868–2878
40. Villalpando S, Gopal J, Balasubramanyam A, Bandi VP, Guntupalli K, Jahoor F: In vivo arginine production and intravascular nitric oxide synthesis in hypotensive sepsis. Am J Clin Nutr 2006, 84:197–203
41. Murugan R, Kellum JA: Acute kidney injury: what's the prognosis? Nat Rev Nephrol 2011, 7:209–217
42. Wan L, Bagshaw SM, Langenberg C, Saotome T, May C, Bellomo R: Pathophysiology of septic acute kidney injury: what do we really know? Crit Care Med 2008, 36:S198–S203
43. Langenberg C, Wan L, Egi M, May CN, Bellomo R: Renal blood flow in experimental septic acute renal failure. Kidney Int 2006, 69:1996–2002
44. Ramchandra R, Wan L, Hood SG, Frithiof R, Bellomo R, May CN: Septic shock induces distinct changes in sympathetic nerve activity to the heart and kidney in conscious sheep. Am J Physiol Regul Integr Comp Physiol 2009, 297:R1247–R1253
45. Brandt S, Regueira T, Bracht H, Porta F, Djafarzadeh S, Takala J, Gorrasi J, Borotto E, Krejci V, Hiltebrand LB, Bruegger LE, Beldi G, Wilkens L, Lepper PM, Kessler U, Jakob SM: Effect of fluid resuscitation on mortality and organ function in experimental sepsis models. Crit Care 2009, 13:R186
46. Chvojka J, Sykora R, Krouzecky A, Radej J, Varnerova V, Karvunidis T, Hes O, Novak I, Radermacher P, Matejovic M: Renal haemodynamic, microcirculatory, metabolic and histopathological responses to peritonitis-induced septic shock in pigs. Crit Care 2008, 12:R164
47. Bradley VE, Shier MR, Lucas CE, Rosenberg IK: Renal hemodynamic response to furosemide in septic and injured patients. Surgery 1976, 79:549–554
48. Brenner M, Schaer GL, Mallory DL, Suffredini AF, Parrillo JE: Detection of renal blood flow abnormalities in septic and critically ill patients using a newly designed indwelling thermodilution renal vein catheter. Chest 1990, 98:170–179
49. Lee WL, Slutsky AS: Sepsis and endothelial permeability. N Engl J Med 2010, 363:689–691
50. Boffa JJ, Just A, Coffman TM, Arendshorst WJ: Thromboxane receptor mediates renal vasoconstriction and contributes to acute renal failure in endotoxemic mice. J Am Soc Nephrol 2004, 15:2358–2365
51. Sutton TA: Alteration of microvascular permeability in acute kidney injury. Microvasc Res 2009, 77:4–7
52. Stearns-Kurosawa DJ, Osuchowski MF, Valentine C, Kurosawa S, Remick DG: The pathogenesis of sepsis. Annu Rev Pathol 2011, 6:19–48
53. Okamoto T, Akaike T, Sawa T, Miyamoto Y, van der Vliet A, Maeda H: Activation of matrix metalloproteinases by peroxynitrite-induced protein S–glutathiolation via disulfide S–oxide formation. J Biol Chem 2001, 276:29596–29602
54. Radi R, Rodriguez M, Castro L, Telleri R: Inhibition of mitochondrial electron transport by peroxynitrite. Arch Biochem Biophys 1994, 308: 89–95
55. Just A, Whitten CL, Arendshorst WJ: Reactive oxygen species participate in acute renal vasoconstrictor responses induced by ETA and ETB receptors. Am J Physiol Renal Physiol 2008, 294:F719–F728
56. Majid DS, Nishiyama A, Jackson KE, Castillo A: Superoxide scavenging attenuates renal responses to ANG II during nitric oxide synthase inhibition in anesthetized dogs. Am J Physiol Renal Physiol 2005, 288:F412–F419
57. Matavelli LC, Kadowitz PJ, Navar LG, Majid DS: Renal hemodynamic and excretory responses to intra-arterial infusion of peroxynitrite in anesthetized rats. Am J Physiol Renal Physiol 2009, 296:F170–F176
58. Nin N, El-Assar M, Sanchez C, Ferruelo A, Sanchez-Ferrer A, Martinez-Caro L, Rojas Y, de Paula M, Hurtado J, Esteban A, Lorente JA: Vascular dysfunction in sepsis: effects of the peroxynitrite decomposition catalyst MnTMPyP. Shock 2011, 36:156–161
59. Tiwari MM, Brock RW, Kaushal GP, Mayeux PR: Disruption of renal peritubular blood flow in lipopolysaccharide-induced renal failure: role of nitric oxide and caspases. Am J Physiol Renal Physiol 2005, 289:F1324–F1332
60. Okusa MD: The changing pattern of acute kidney injury: from one to multiple organ failure. Contrib Nephrol 2010, 165:153–158
61. Crimi E, Sica V, Williams-Ignarro S, Zhang H, Slutsky AS, Ignarro LJ, Napoli C: The role of oxidative stress in adult critical care. Free Rad Biol Med 2006, 40:398–406
62. Nilakantan V, Liang HL, Rajesh S, Mortensen J, Chandran K: Time-dependent protective effects of manganese(III) tetrakis (1-methyl-4-pyridyl) porphyrin on mitochondrial function following renal ischemia-reperfusion injury. Free Radic Res 2010, 44:773–782
63. Doi K, Hu X, Yuen PS, Leelahavanichkul A, Yasuda H, Kim SM, Schnermann J, Jonassen TE, Frokiaer J, Nielsen S, Star RA: AP214, an analogue of alpha-melanocyte–stimulating hormone, ameliorates sepsis-induced acute kidney injury and mortality. Kidney Int 2008, 73:1266–1274
64. Leelahavanichkul A, Yasuda H, Doi K, Hu X, Zhou H, Yuen PS, Star RA: Methyl-2-acetamidoacrylate, an ethyl pyruvate analog, decreases sepsis-induced acute kidney injury in mice. Am J Physiol Renal Physiol 2008, 295:F1825–F1835
65. Holthoff JH, Wang Z, Seely KA, Gokden N, Mayeux PR: Resveratrol improves renal microcirculation, protects the tubular epithelium, and prolongs survival in a mouse model of sepsis-induced acute kidney injury. Kidney Int 2011, doi:10.1038/ki.2011.347